SINTEF
PROCEEDINGS
2

Proceedings of the 12th International Conference on Computational Fluid Dynamics in the Oil & Gas, Metallurgical and Process Industries

Progress in Applied CFD – CFD2017

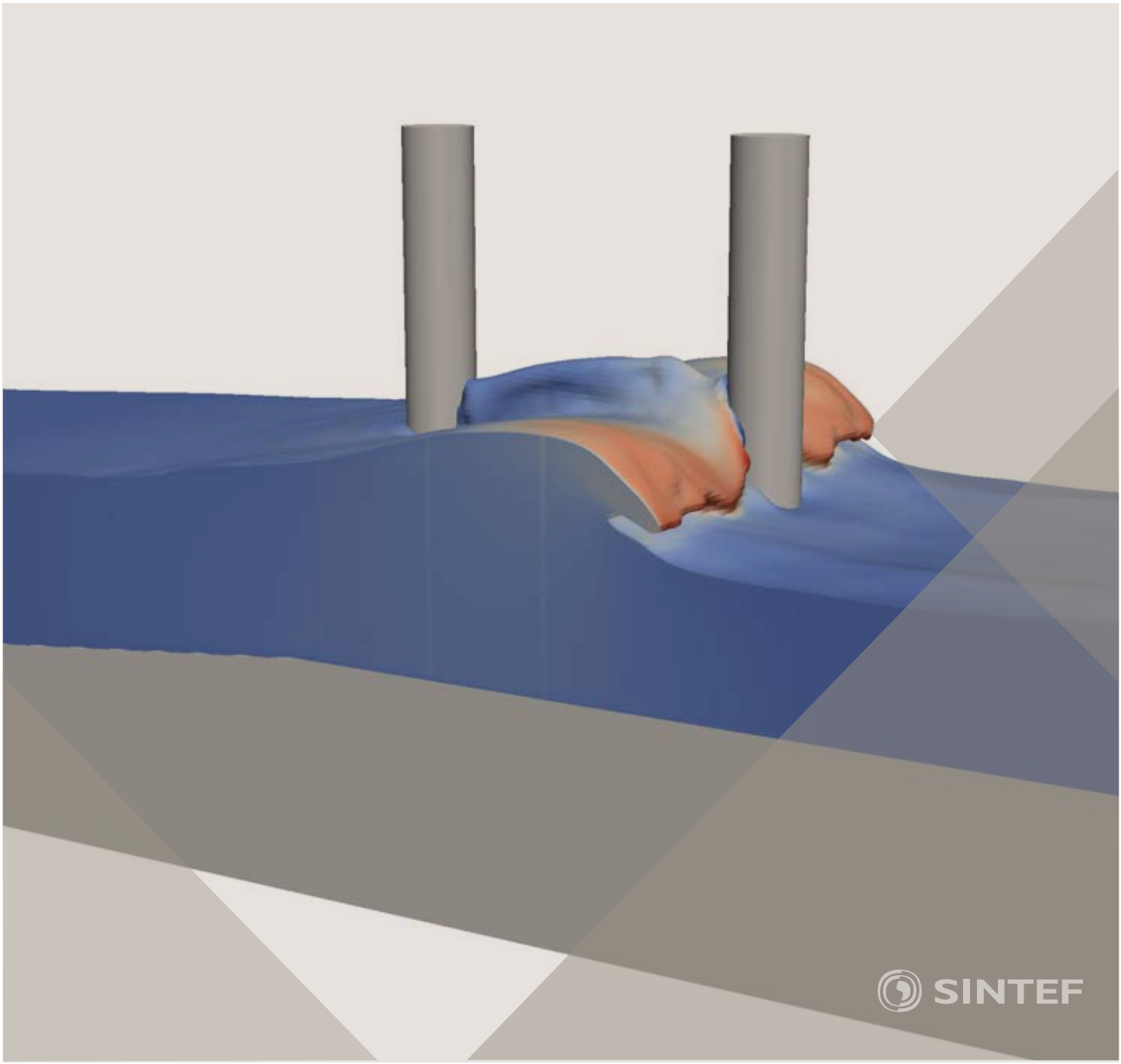

SINTEF Proceedings

Editors:
Jan Erik Olsen and Stein Tore Johansen

Progress in Applied CFD – CFD2017

Proceedings of the 12th International Conference on Computational Fluid Dynamics in the Oil & Gas, Metallurgical and Process Industries

SINTEF Academic Press

SINTEF Proceedings no 2
Editors: Jan Erik Olsen and Stein Tore Johansen
Progress in Applied CFD – CFD2017
Selected papers from 10th International Conference on Computational Fluid Dynamics in the Oil & Gas, Metallurgical and Process Industries

Key words:
CFD, Flow, Modelling

Cover, illustration: Arun Kamath

ISSN 2387-4295 (online)
ISBN 978-82-536-1544-8 (pdf)

SINTEF Academic Press
Address: Forskningsveien 3 B
PO Box 124 Blindern
N-0314 OSLO
Tel: +47 73 59 30 00
Fax: +47 22 96 55 08

www.sintef.no/byggforsk
www.sintefbok.no

SINTEF Proceedings
SINTEF Proceedings is a serial publication for peer-reviewed conference proceedings on a variety of scientific topics.
The processes of peer-reviewing of papers published in SINTEF Proceedings are administered by the conference organizers and proceedings editors. Detailed procedures will vary according to custom and practice in each scientific community.

PREFACE

This book contains all manuscripts approved by the reviewers and the organizing committee of the 12th International Conference on Computational Fluid Dynamics in the Oil & Gas, Metallurgical and Process Industries. The conference was hosted by SINTEF in Trondheim in May/June 2017 and is also known as CFD2017 for short. The conference series was initiated by CSIRO and Phil Schwarz in 1997. So far the conference has been alternating between CSIRO in Melbourne and SINTEF in Trondheim. The conferences focuses on the application of CFD in the oil and gas industries, metal production, mineral processing, power generation, chemicals and other process industries. In addition pragmatic modelling concepts and bio-mechanical applications have become an important part of the conference. The papers in this book demonstrate the current progress in applied CFD.

The conference papers undergo a review process involving two experts. Only papers accepted by the reviewers are included in the proceedings. 108 contributions were presented at the conference together with six keynote presentations. A majority of these contributions are presented by their manuscript in this collection (a few were granted to present without an accompanying manuscript).

The organizing committee would like to thank everyone who has helped with review of manuscripts, all those who helped to promote the conference and all authors who have submitted scientific contributions. We are also grateful for the support from the conference sponsors: ANSYS, SFI Metal Production and NanoSim.

Stein Tore Johansen & Jan Erik Olsen

Organizing committee:

Conference chairman: Prof. Stein Tore Johansen
Conference coordinator: Dr. Jan Erik Olsen
Dr. Bernhard Müller
Dr.Sigrid Karstad Dahl
Dr.Shahriar Amini
Dr.Ernst Meese
Dr.Josip Zoric
Dr.Jannike Solsvik
Dr.Peter Witt

Scientific committee:

Stein Tore Johansen, SINTEF/NTNU
Bernhard Müller, NTNU
Phil Schwarz, CSIRO
Akio Tomiyama, Kobe University
Hans Kuipers, Eindhoven University of Technology
Jinghai Li, Chinese Academy of Science
Markus Braun, Ansys
Simon Lo, CD-adapco
Patrick Segers, Universiteit Gent
Jiyuan Tu, RMIT
Jos Derksen, University of Aberdeen
Dmitry Eskin, Schlumberger-Doll Research
Pär Jönsson, KTH
Stefan Pirker, Johannes Kepler University
Josip Zoric, SINTEF

CONTENTS

NUMERICAL STUDY OF COAL PARTICLE GASIFICATION UP TO REYNOLDS NUMBERS OF 1000

Sebastian KRIEBITZSCH[1]*, **Andreas RICHTER**[1]†
[1]CIC Virtuhcon, Institute of Energy Process Engineering and Chemical Engineering,
TU Bergakademie Freiberg, 09599 Freiberg, GERMANY

* E-mail: sebastian.kriebitzsch@vtc.tu-freiberg.de
† E-mail: a.richter@vtc.tu-freiberg.de

ABSTRACT
The influence of turbulent structures on the gasification of coal particles, in particular on the char consumption and surface temperature, is studied . Existing submodels for char gasification are mainly based on results for laminar flow only, therefore the capability of these models to predict gasification at higher particle Reynolds numbers is evaluated using the simulation results. Two representative scenarios were studied: the gasification of a 2 mm particle at atmospheric pressure in a O_2/CO_2/H_2O atmosphere at 2006 K and the gasification of a 263 µm particle at 30 bar in a different O_2/CO_2/H_2O atmosphere at 1480 K. The simulation conditions were based on data obtained from the simulations of two different entrained-flow gasifiers. ANSYS Fluent™ was used to solve the Navier-Stokes equations for the flow field coupled with energy and species conservation equations. The model for the reaction system incorporates six gaseous chemical species H_2, O_2, CO, CO_2, H_2O, N_2 and solid carbon. A semi-global reaction mechanism was applied for the homogeneous gas-phase reactions and the water gas reaction, the Boudouard reaction and the oxidation of carbon to carbon monoxide were considered as heterogeneous gas-solid reactions. In the present work it is shown how the reaction zone is modified due to the change in wake structure, the impact of the turbulent effects on the overall carbon conversion rate are discussed, and hints how to adjust existing submodels to correctly predict char conversion at high particle Reynolds numbers are given.

Keywords: CFD, gasification, turbulence, heterogeneous reactions.

NOMENCLATURE

Greek Symbols
λ_{ij} stochiometric coefficient of species i in reaction j, $[-]$
θ empirical factor, $[-]$
ν kinematic viscosity, $[m^2/s]$

Latin Symbols
c_i molar concentration of species i, $[kmol/m^3]$.
d_P particle diameter, $[m]$.
k reaction rate constant, in SI units.
$k\infty$ pre-exponential factor, in SI units.
n exponent of power law kinetic rate equations, $[-]$.
p_i partial pressure of species i, $[Pa]$.
p_{op} operating pressure, $[Pa]$.
r molar reaction rate, $[kmol/m^3 s]$.
u maginitude of velocity, $[m/s]$.
D_{eff} effective diffusion coefficient in a porous medium, $[m^2/s]$.
E_a activation energy, $[J/kmol]$.
K inhibition constant, $[1/Pa]$.
R universal gas constant, $[J/kmol \cdot K]$.
Re particle Reynolds number: $Re = u_{in} \cdot d_P/\nu$, $[-]$.
S_V Specific surface area per volume, $[m^2/m^3]$.
X char conversion, $[-]$.
Y mass fraction, $[-]$.

Sub/superscripts
in at the inlet boundary

INTRODUCTION

Due to the multiscale character of coal combustion and gasification processes, the use of sub-models describing particle-gas interaction is unavoidable, and the correct prediction of the burning rate and the particle temperature based on this sub-models is an essential part of successfully modeling of such reactors (Edge *et al.*, 2011; Schulze *et al.*, 2013; Richter *et al.*, 2016). An analysis of existing computational burnout sub-models reveals that e. g. the influence of particle velocity on carbon consumption and particle temperature is not well understood. Thus, particle-resolved numerical simulations of single burning particles can highlight different physical phenomena and correlations and therefore they can help to better understand the complex combustion physics. Examples for this approach are given in Refs. (Lee *et al.*, 1996; Higuera, 2008; Kestel *et al.*, 2012; Richter *et al.*, 2013, 2015; Wittig *et al.*, 2016).
To the authors best knowledge almost all single-particle studies published in literature considered laminar flow regimes only and most consider only one heterogeneous reaction i.e. Boudouard, watergas or carbon oxidation. In different technological applications much larger particle Reynolds numbers are possible and all three above mentioned reactions proceed in parallel. For that reason the char-particle burnout corresponding to turbulent flow up to particle Reynolds number equals 1000 in two different O_2/CO_2/H_2O atmospheres is investigated. At these Reynolds numbers time periodicity and the planar symmetry of the vortex shedding are lost and the wake becomes turbulent (Jones and Clarke, 2008; Campregher *et al.*, 2009) . The operating conditions, that means pressure, temperature and gas phase composition, are based

on data obtained from simulations of two different entrained-flow gasifiers.

MODEL DESCRIPTION

The gasification is studied for a single spherical particle in embedded in a large domain as schematically shown in Figure 1. As the heterogeneous reaction time scales are much

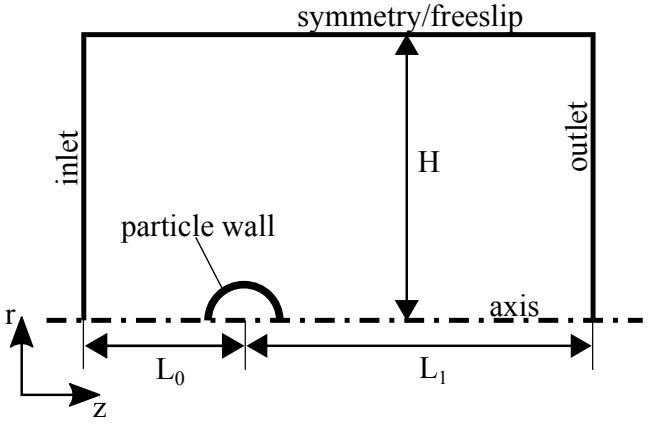

Figure 1: Schematic drawing of the 2D domain used in the simulations.

larger than the flow time scales (Sundaresan and Amundson, 1980; Richter *et al.*, 2013), the pseudo-steady state approach was assumed valid, hence no particle-shrinking was taken into account and the steady-state form of the governing equations are solved. Indeed this assumption is confirmed from the simulations results. The lowest value of the ratio of carbon consumption time scale and fluid time scale is found to be of the order $O(10)$, but in most of the cases it is higher. Fluid flow is modelled coupled with species and energy transport as well as coupled with heat conduction inside the solid particle. Buoyancy effects are neglected, hence gravity is set to zero but the density still varies due to e.g. changes in temperature. Turbulence is taken into account using the k-ω-SST model in the steady RANS simulations for particle Reynolds numbers larger than $Re = 200$. The Maxwell-Stefan equations are used to describe diffusional mass flux in the multi-component gas mixture and gas-gas radiation is included via the P1 radiation model. The heterogeneous reactions are assumed to take place on the outer particle surface only, however the internal structure of the char particle is considered through an effectiveness factor, which is defined in the next section. The gas phase is modelled as an incompressible ideal gas and all physical properties of the components are modelled using polynomial expressions or kinetic theory. The chemical system incorporates pure carbon as solid and H_2, O_2, H_2O, CO, and CO_2 as gaseous species. Details of the finite-rate chemical mechanism are discussed in the next section. The process and inlet condition for the two different cases studied in this work are shown in Table 1. Uniform profiles are prescribed for velocity, temperature and species concentrations at the inlet.

Chemical reactions

The semi-global mechanism to describe the homogeneous gas phase reactions are modelled using a mechanism proposed by Jones and Lindstedt (1988):

$$H_2 + 0.5\,O_2 \rightleftharpoons H_2O \qquad \text{(R1)}$$
$$CO + H_2O \rightleftharpoons CO_2 + H_2, \qquad \text{(R2)}$$

	case	
	1	2
d_P/m	$2 \cdot 10^{-3}$	$0.263 \cdot 10^{-3}$
P_{op}/bar	1.013	30
T_{in}/K	2006	1480
Re_{in}	1 – 500	1 – 1000
$u_{in}/\frac{m}{s}$	0.1932 – 95.58	0.03192 – 31.92
$Y_{CO_2,in}$	0.223	0.223
$Y_{H_2O,in}$	0.123	0.221
$Y_{O_2,in}$	0.366	0.187

Table 1: Process and inlet conditions for both cases considered.

however with modified reaction rate kinetics for the hydrogen oxidation R1 as used by Kim *et al.* (2008). A simple power law is used to compute the reaction rates for R1

$$r_{R1} = k_\infty \cdot \exp\left\{-\frac{E_a}{R \cdot T}\right\} \cdot c_{O_2}^{0.5} \cdot c_{H_2} \qquad (1)$$

and for R2:

$$r_{R2} = k_\infty \cdot \exp\left\{-\frac{E_a}{R \cdot T}\right\} \cdot c_{CO} \cdot c_{H_2O}, \qquad (2)$$

	k_∞	$E_a/(J/kmol)$
R1	$5.69 \cdot 10^{11}$	$1.465 \cdot 10^8$
R2	$2.75 \cdot 10^9$	$8.368 \cdot 10^7$

Table 2: Kinetic constants for the gas phase reactions.

The Boudouard and water-gas reaction as well as the oxidation of the carbon are considered as heterogeneous reactions of the particles with the gas phase:

$$C + CO_2 \longrightarrow 2\,CO \qquad \text{(R3)}$$
$$C + H_2O \longrightarrow H_2 + CO \qquad \text{(R4)}$$
$$2\,C + O_2 \longrightarrow 2CO \qquad \text{(R5)}$$

Different sets of kinetic rate equations are used for atmospheric conditions (case 1) and pressurized case (case 2). For the atmospheric conditions of case 1 the model for the effective reaction rates proposed by Vascellari *et al.* (2014) is used:

$$r_{R3,1} = \theta(X) \cdot k_\infty \cdot \exp\left\{-\frac{E_a}{R \cdot T}\right\} \cdot \frac{p_{CO_2}^n}{1 + K_{CO} \cdot p_{CO}}, \qquad (3)$$

$$r_{R4,1} = \theta(X) \cdot k_\infty \cdot \exp\left\{-\frac{E_{a,R4}}{R \cdot T}\right\} \cdot \frac{p_{H_2O}^n}{1 + K_{H_2} \cdot p_{H_2}}, \qquad (4)$$

$$r_{R5,1} = \theta(X) \cdot k_\infty \cdot \exp\left\{-\frac{E_a}{R \cdot T}\right\} \cdot p_{O_2}^n, \qquad (5)$$

The rate constants are taken from Richter *et al.* (2016) and are given in Table 3.
$\theta(X)$ is an empirical factor to account for the inner structure of the particle, which is calculated as described in Vascellari *et al.* (2014).

	$k_\infty/\left(^{kmol}/_{(m^3 s Pa^n)}\right)$	$E_a/\left(^{J}/_{kmol}\right)$	n	$K/\left(^{1}/_{Pa}\right)$
R3	$9.04 \cdot 10^3$	$1.3063 \cdot 10^8$	0.76	$5{,}47 \cdot 10^{-6}$
R4	7.30	$1.0676 \cdot 10^8$	0.97	$3.19 \cdot 10^{-7}$
R5	$1.77 \cdot 10^4$	$1.771 \cdot 10^8$	1	

Table 3: Kinetic constants for the effective reaction rates of the boudouard, water gas and oxidation reactions from Richter *et al.* (2016).

At 30bar operating pressure (case 2), the intrinsic reaction rate data of Hla *et al.* (2007) is taken and modified with an effectiveness factor η_P to account for the transport resistances inside the particle. Hence the effective reaction rates are:

$$r_{R3,2} = \eta_{P,CO_2} \cdot S_V \cdot k_\infty \cdot \exp\left\{-\frac{E_a}{R \cdot T}\right\} \cdot p^n_{CO_2}, \quad (6)$$

$$r_{R4,2} = \eta_{P,H_2O} \cdot S_V \cdot k_\infty \cdot \exp\left\{-\frac{E_a}{R \cdot T}\right\} \cdot p^n_{H_2O}, \quad (7)$$

$$r_{R5,2} = \eta_{P,O_2} \cdot S_V \cdot k_\infty \cdot \exp\left\{-\frac{E_a}{R \cdot T}\right\} \cdot p^n_{O_2}, \quad (8)$$

The rate constants are given in Table 4.

	$k_\infty/\left(^{kmol}/_{(m^2 s Pa^n)}\right)$	$E_a/\left(^{J}/_{kmol}\right)$	n
R3	$3.331 \cdot 10^{-2}$	$2.11 \cdot 10^8$	0.4
R4	2.485	$2.31 \cdot 10^8$	0.4
R5	$1.236 \cdot 10^{-3}$	$1.36 \cdot 10^8$	0.8

Table 4: Kinetic constants for the intrinsic reaction rates of the boudouard, water gas and oxidation reactions fro Hla *et al.* (2007) for coal CRC272.

The effectivity for the species i and reaction j is estimated as

$$\eta_j(\Phi_{ij}) = \frac{1}{\Phi_{ij}} \left(\frac{1}{\tanh(3\Phi_{ij})} - \frac{1}{3\Phi_{ij}} \right), \quad (9)$$

using a generalized Thiele modules Φ_{ij} which is (almost) independent of the particle shape. For a power-law kinetic reaction rate defined it is defined as:

$$\Phi_{ij} = \frac{V_P}{S_P} \sqrt{\frac{n+1}{2} \frac{\lambda_{ij} \cdot k_{\infty,j} \cdot \exp\left\{-\frac{E_{a,j}}{R \cdot T}\right\} \cdot S_V \cdot p_i^{n-1}}{D_{eff,i}}} \quad (10)$$

Simulation settings

ANSYS Fluent™ V 17.2 was used to solve the Navier-Stokes equations coupled with species and energy transport. The pressure based solver was used and the differential equations where discretized using second order schemes in space and time. Only the convective fluxes where discretized with a third-order MUSCL scheme in the steady RANS simulations. For the 2D-axisymmetric simulations the domain extends $L_0 = 30 d_P$ in upstream, $L_1 = 100 d_P$ in downstream and $H = 40 d_P$ in radial direction. Based on the 2D results, the 3D-domain has been chosen slightly smaller. The cuboid extends $L_0 = 8 d_P$ in upstream, $L_1 = 24 d_P$ in downstream and $H = 8 d_p$ in the lateral directions. The number of grid cells used is 27,750 for the 2D simulations and 4,085,112 for the 3D simulations. Grid-independence has been confirmed in previous investigations by Richter *et al.* (2015, 2016). A comprehensive validation of the model setup against different experimental data is given in Richter *et al.* (2013).

RESULTS

In order to reduce the computational effort, as the final aim of this research is to study gasification in high detail with three-dimensional transient LES simulations, a semi-global mechanism is used in this work. Hence for comparison simulations have been done with the detailed drm22-mechanism proposed by Kazakov and Frenklach (1994). Results for the atmospheric case at $Re = 500$ are shown in Figure 2 and for the pressurized case at $Re = 1000$ in Figure 3. The general features of the flame structure are repro-

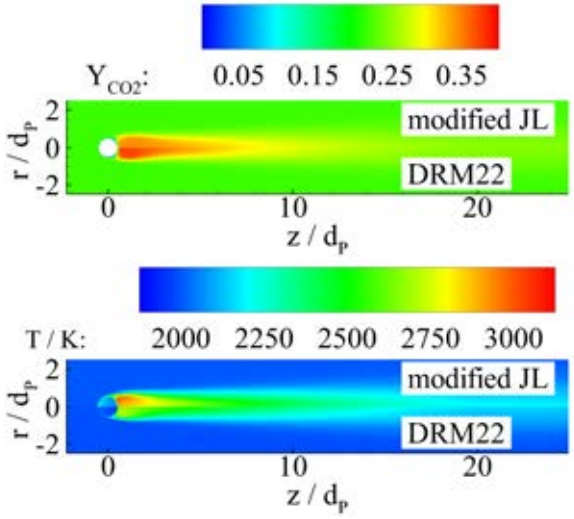

Figure 2: Contours of the mass fraction Y_{CO_2} and Temperature T at $Re = 500$ for case 1. The upper half shows results obtained with the semi-global mechanism proposed by Kim *et al.* (2008), which is used in this work, and the lower half results obtained with the detailed chemical mechanism drm22 by Kazakov and Frenklach (1994).

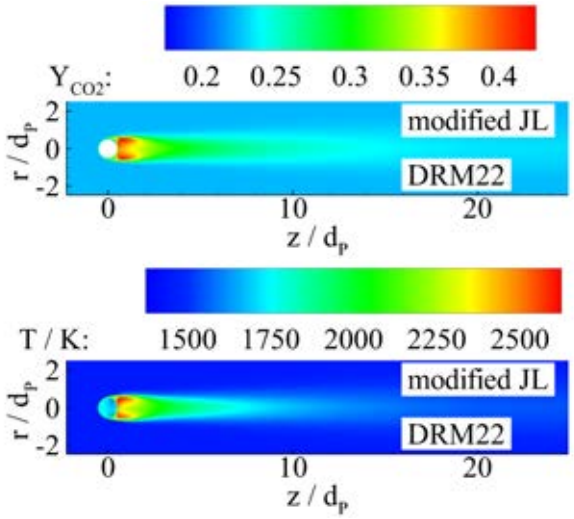

Figure 3: As in Figure 2, however for case 2 at $Re = 1000$.

duced with the semi-global mechanism, however some differences can be observed in particular in the contours shown for the atmospheric case 1. The maximum temperature is higher and the high temperature zone is more pronounced for the semi-global mechanism. The maximum CO_2 mass fraction is larger when using the detailed mechanism, however the shape of the CO_2-rich zone is similar. The higher CO_2 mass fraction can be explained by the simplified semi-global mechanism, which only considers the hydrogen oxi-

dation R1 and the water-gas shift reaction R2, whereas the detailed DRM22 mechanism also includes the oxidation of CO to CO_2. Under the pressurized conditions of case 2 the differences in the results using the different mechanisms are less pronounced. Please note that the same gas phase mechanisms have been used in both cases, only the heterogeneous gas-surface reactions and the operating conditions are changed. The flame zone is slightly larger for the semi-global mechanism and the maximum temperature is slightly higher. Secondly the influence of turbulence on the gasification is studied.A qualitative comparison is presented in Figure 4, which shows the contours of the temperature for case 2 at different particle Reynolds-numbers. A similar picture is obtained for the atmospheric pressure case 1. The maximum temperature remains almost constant, however the shape and size of the flame zone significantly change with increasing particle Reynolds number. Fully engulfing the particle at low particle Reynolds numbers, the flame zone is gradually thinning with particle Reynolds number accompanied by an increasing fore-aft asymmetry such that a separated reaction zone persists at higher particle Reynolds numbers.

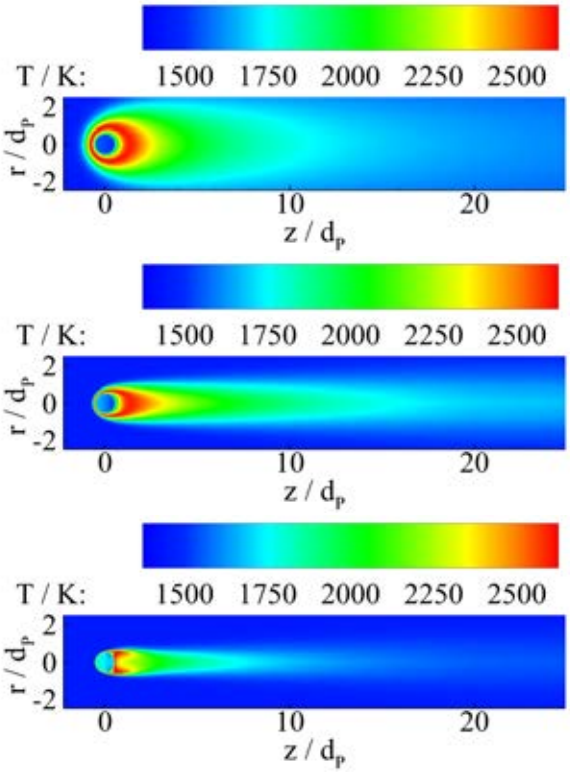

Figure 4: Contours of the temperature T for different particle Reynolds numbers. From top to bottom: $Re = 10, 100, 1000$ for case 2.

Quantitative data are given in Figures 5 and 6, which show the average temperature on the particle surface and the average carbon mass flux for case 1 and for case 2, respectively. Results are presented for 2D-axisymmetric RANS simulations and for 3D RANS simulations at the highest particle Reynolds number. The differences between the 2D and the 3D results are small, which shows that the 2D axisymmetric assumption is justified. Initially the eddy dissipation concept (EDC) model for turbulence-chemistry interaction has been used for all simulations with $Re > 200$. However in the graphs of the average surface temperature and also the species mass fractions a sudden jump has been found in the results rather than a smooth transition, which is considered

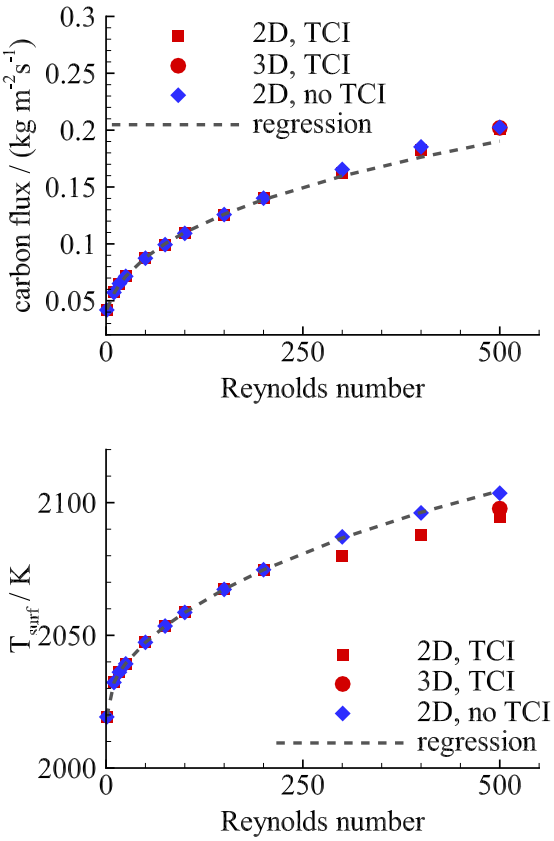

Figure 5: Carbon mass flux and temperature as a function of the particle Reynolds number for case 1.TCI denotes simulations using the eddy dissipation concept (EDC) to account for turbulence-chemistry interaction.

non-physical. The red squares in the graphs for the surface temperature of Figures 5 and 6 show these findings. As the EDC model has originally been developed for highly turbulent flows, this model is considered the main suspect for the observed non-physical behaviour. Hence simulations with exactly the same simulations have been done, only with the turbulence-chemistry model turned off. The results are shown by the blue symbols in Figures 5 and 6. The jump has disappeared and a continuous change of surface temperature with particle Reynolds number can be seen. The contours of CO_2 mass fraction and temperature shown in Figure 7 for case 2 at $Re = 1000$ shed some lights on this question. Note that similar results are found for case 1 and for different particle Reynolds numbers. Qualitatively similar results are obtained for the simulations with and without turbulence-chemistry interaction turned on, only a higher temperatures and a higher CO_2 mass fraction are observed in the very thin flame zone close to the particle surface. However in this region the flow conditions are laminar and the grid is fine enough such that all scales are resolved. Hence the EDC model, which is based on the assumption of fully turbulent conditions, too strongly dampens the reactions which leads to the non-physical jump in the results. The carbon flux on the other hand is almost unaffected by the use of the EDC model and no clear jump is visible.

Finally, the dashed-lines in Figures 5 and 6 are a regression based on the laminar results, i.e. for $Re <= 200$. One sees that the extrapolation of the laminar results to higher particle Reynolds number still give a reasonable prediction of the carbon consumption, the maximum difference is about 10%.

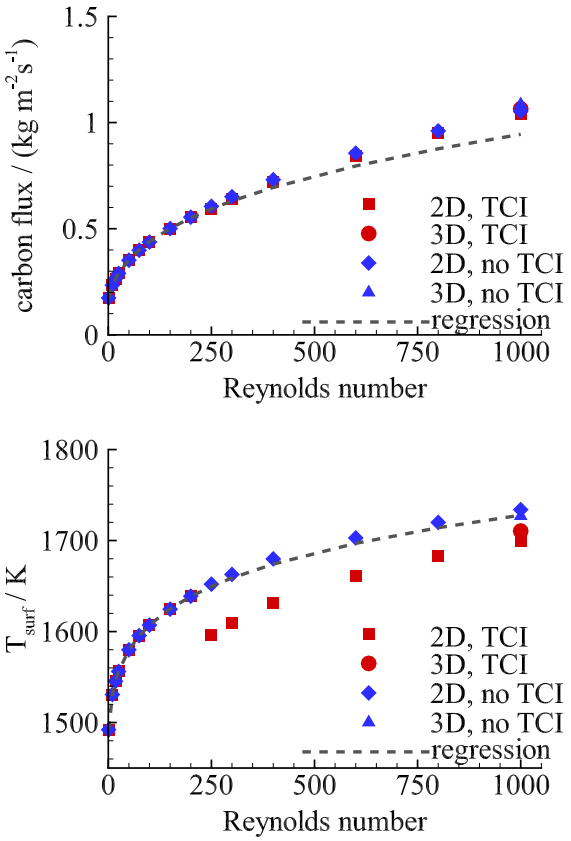

Figure 6: Carbon mass flux and temperature as a function of the particle Reynolds number for case 2.TCI denotes simulations using the eddy dissipation concept (EDC) to account for turbulence-chemistry interaction.

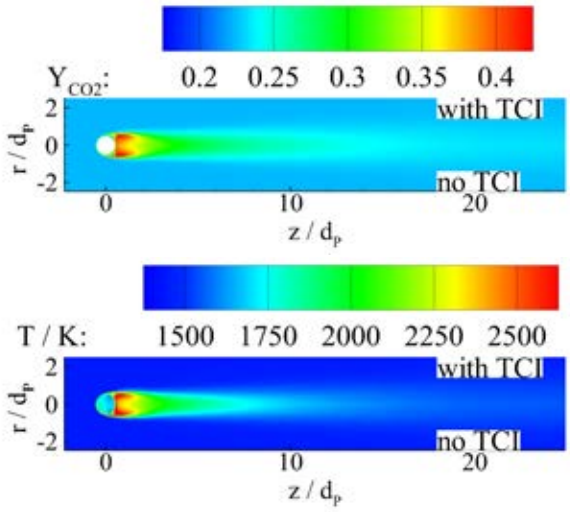

Figure 7: Influence of turbulence-chemistry interaction for case 2 at $Re = 1000$.The upper half shows results obtained using the EDC model for turbulent-chemistry interaction, which is turned of in the lower half

CONCLUSIONS AND OUTLOOK

In this work the interplay between a turbulent chemically-reacting flow and heterogeneous gasification and combustion on a particle surface has been studied. It has been shown that the main features of the flame-zone are well captured using a simple semi-global gas phase mechanism and that the use of axisymmetric 2D simulations is justified. The use of the EDC turbulence-chemistry interaction leads to a too strong damping of the gas phase reactions near the particles, which strongly affects the surface temperature and species distribution, however the total carbon consumption rate is only mildly influenced. The reaction zone is strongly modified due to the change in wake structure. From engulfing the whole particle at low particle Reynolds numbers, a increasing fore-aft asymmetry has been found which lead to a separated flame zone at high particle Reynolds numbers. Despite the strong changes in the shape of the reaction zone, extrapolation of the laminar results into the turbulent regime gives a reasonable prediction of the carbon consumption rate and the surface temperature. This shows that models, based on laminar flow conditions, which are capable of capturing the fore-aft symmetry, can at least as a first estimate be used to also model gasification at larger particle Reynolds numbers. Finally as a completion of this work, currently 3D LES simulations are under way to study the effect of turbulent fluctuations on the overall carbon consumptions rate.

REFERENCES

CAMPREGHER, R., MILITZER, J., MANSUR, S.S. and DA SILVEIRA NETO, A. (2009). "Computations of the flow past a still sphere at moderate reynolds numbers using and immersed boundary method". *J. Braz. Soc. Mech. Sci. & Eng*, **31**, 344–352.

EDGE, P., GHAREBAGHI, M., IRONS, R., PORTER, R., PORTER, R.T.J., POURKASHANIAN, M., SMITH, D., STEPHENSON, P. and WILLIAMS, A. (2011). "Combustion modelling opportunities and challenges for oxy-coal carbon capture technology". *Chem. Eng. Res. Des.*, **89**, 1470–1493.

HIGUERA, F.J. (2008). "Combustion of a coal char particle in a stream of dry gas". *Combust. & Flame*, **152**, 230–244.

HLA, S.S., HARRIS, D. and ROBERTS, D. (2007). "Gasification conversion model – PEFR". Research report 80. Cooperative research centre for coal in suistainable development.

JONES, D.A. and CLARKE, D.B. (2008). "Simulations of flow past a sphere using the fluent code". Technical report. Austral. Gov., Dep. of Def., Def. Sc. and Techn. Org.

JONES, W.P. and LINDSTEDT, R.P. (1988). "Global reaction schemes for hydrocarbon combustion". *Combust. & Flame*, **73**, 233–249.

KAZAKOV, A. and FRENKLACH, M. (1994). "Reduced reaction sets based on gri-mech 1.2". http://www.me.berkeley.edu/drm/.

KESTEL, M., NIKRITYUK, P.A., HENNIG, O. and HASSE, C. (2012). "Numerical study of the partial oxidation of a coal particle in steam and dry air atmospheres". *IMA J. Appl. Math.*, **77**, 32–46.

KIM, J.P., SCHNELL, U. and SCHEFFKNECHT, G. (2008). "Comparison of different global reaction mechanisms for MILD combustion of natural gas". *Comb. Sci. Technol.*, **180**, 565–592.

LEE, J., TOMBOULIDES, A.G., ORSZAG, S.A., YETTER, R.A. and DRYER, F.L. (1996). "A transient two-dimensional chemically reactive flow model: Fuel particle combustion in a nonquiescent environment". *Proc. Combust. Inst.*, **26**, 3059–3065.

RICHTER, A., NIKRITYUK, P.A. and KESTEL, M. (2013). "Numerical investigation of a chemically reacting carbon particle moving in a hot O2/CO2 atmosphere". *Ind. Eng. Chem.*, **52**, 5815–5824.

RICHTER, A., NIKRITYUK, P.A. and MEYER, B. (2015). "Three-dimensional calculation of a chemically reacting porous particle moving in a hot O2/CO2 atmosphere". *Int. J. Heat Mass Transfer*, **83**, 244–258.

RICHTER, A., VASCELLARI, M., NIKRITYUK, P.A. and HASSE, C. (2016). "Detailed analysis of reacting particles in an entrained-flow gasifier". *Fuel Process. Technol.*, **144**, 95–108.

SCHULZE, S., KESTEL, M., NIKRITYUK, P.A. and SAFRONOV, D. (2013). "From detailed description of chemical reacting carbon particles to subgrid models for CFD". *Oil Gas Sci. Technol.*, **68**, 1007–1026.

SUNDARESAN, S. and AMUNDSON, N.R. (1980). "Diffusion and reaction in a stagnant boundary layer about a carbon particle. 5. pseudo-steady-state structure and parameter sensitivity". *Ind. Eng. Chem. Fundam.*, **19**, 344–351.

VASCELLARI, M., ARORA, R. and HASSE, C. (2014). "Simulation of entrained flow gasification with advanced coal conversion submodels. part 2: Char conversion". *Fuel*, **118**, 369 – 384.

WITTIG, K., NIKRITYUK, P.A., SCHULZE, S. and RICHTER, A. (2016). "Three-dimensional modeling of porosity development during the gasification of a char particle". *AICJE J.*, available online.